Nonlinear Layer-by-Layer Films: Effects of Chain Diffusivity on Film Structure and Swelling

Victor Selin,[†] John F. Ankner,[‡] and Svetlana A. Sukhishvili,[†]

[†]*Department of Materials Science & Engineering, Texas A&M University, College Station, Texas 77843, United States*

[‡]*Spallation Neutron Source, Oak Ridge National Laboratory, Oak Ridge, Tennessee 37831, United States*

Nonlinear Layer-by-Layer Films: Effects of Chain Diffusivity on Film Structure and Swelling

Victor Selin[1], John F. Ankner[2], and Svetlana A. Sukhishvili[1]*

[1] *Department of Materials Science & Engineering, Texas A&M University, College Station, Texas 77843, USA*

[2]*Spallation Neutron Source, Oak Ridge National Laboratory, Oak Ridge, Tennessee 37831, USA*

Abstract

We report on the role of molecular diffusivity in the formation of nonlinearly growing polyelectrolyte multilayers (*nl*PEMs). Electrostatically bound polyelectrolyte multilayers were assembled from poly(methacrylic acid) (PMAA) as a polyanion and quaternized poly-2-(dimethylamino)ethyl methacrylate (QPC) as a polycation. Film growth as measured by ellipsometry was strongly dependent on the time allowed for each polymer deposition step, suggesting that the diffusivities of the components are crucial in controlling the rate of film growth. Uptake of polyelectrolytes within *nl*PEMs was relatively slow, and occurred on time scales ranging from minutes to hours, depending on the film thickness. Spectroscopic ellipsometry measurements with *nl*PEM films exposed to aqueous solutions exhibited high (several-fold) degrees of film swelling, and different swelling values for films exposed to QPC or PMAA solutions. FTIR spectroscopy showed that the average ionization of film-assembled PMAA increased upon binding of QPC, and decreased upon binding of PMAA, in agreement with the charge regulation mechanism for weak polyelectrolytes. The use of neutron reflectometry (NR) enabled quantification of chain intermixing within the film, which was drastically enhanced when longer times were allowed for polyelectrolyte deposition. Diffusion coefficients of the polycation derived from the uptake rates of deuterated chains within hydrogenated films were of the order of 10^{-14} cm^2/s, *i.e.* 5 to 6 orders of magnitude smaller than those found for diffusion of free polymer chains in solution. Exchange of the polymer solutions to buffer inhibited film intermixing. Taken together, these results contribute to understanding the mechanism of the growth of nonlinear polyelectrolyte multilayers and demonstrate the possibility of controlling film intermixing, which is highly desirable for potential future applications.

Introduction

The layer-by-layer (LbL) technique presents a versatile way to coat the surfaces of a diverse range of materials with nanoscopically structured films.[1] LbL-deposited polyelectrolyte multilayers (PEMs) have found a number of applications, showing particular promise for surface functionalization of biomedical devices to control cell adhesion, antibacterial properties and localized delivery of bioactive molecules.[2,3,4] For the use of LbL films as drug-delivery coatings, the overall capacity for loading bioactive molecules is especially important, and micron-thick rather than ultrathin films are optimal. At the same time, it is desirable to control film stratification to enable sequential delivery of multiple functional molecules.[5] Addressing this challenge requires detailed understanding of LbL films that grow non-nonlinearly and feature more mass deposited in fewer steps compared to films grown linearly.[6] The designation of PEMs as either linear or nonlinear (*l*PEMs and *nl*PEMs, respectively) refers to the shape of their growth curves, wherein total film thickness is plotted *vs*. deposition time or number of deposition steps. The rate of deposition and whether it increases with time is determined by the strength of binding between polyelectrolyte components.[7,8] Linear film growth is typical for strongly bound polyelectrolytes, and exhibits a constant increment in mass increase per deposition step and fast saturation of mass at each deposition step. In contrast, accelerated, non-linear (also often called "exponential") film growth is mostly observed for systems with weak binding between polyelectrolyte chains.[9-11] Thicker films are formed as mobile polymer chains do not just bind at the film surface, but penetrate deeper within films.[12,13] Recently, differing growth kinetics for linear and nonlinear films was reported for a clay-containing system, with a strong increase in film thickness with deposition time observed for weakly bound polymer/clay pairs, and film thickness being almost independent of deposition time for strongly interacting polymer-clay pairs.[14] Chain mobility and film growth modes are dependent on polyelectrolyte type and chain rigidity, [15] and can be modulated by concentration and type of salt,[16,17-19] temperature,[20,21] or solution pH. [22,23]

Films which grow nonlinearly (exponentially) were first seen in pairs of weakly associating biological polyelectrolytes. [6,11-13] Diffusion of at least one of polyelectrolytes within the film was established as a condition necessary to observe exponential film growth, and a model suggesting "in-and-out" free diffusion of polyelectrolyte chains between film and solution at alternating film deposition cycles was developed.[11-13] Diffusion of polyelectrolyte chains being

limited to a zone close to the film-solution interface was also suggested, and used to explain a transition from exponential to linear film growth after a large number of deposition steps.[24] The "in-and-out" model is widely but not universally accepted; some groups propose an alternative "dendritic and island" explanation for exponential film growth.[25] Overall, in spite of an increasing number of experimental reports of nonlinear growth in LbL films, the structure and dynamics of these films are still poorly understood. The only existing mathematical model of exponential film growth[26] assumes diffusion of polyelectrolytes throughout PEMs and consequent film swelling. To assess the validity of such assumptions, it is necessary to measure and quantify chain diffusion and layer intermixing in nonlinear PEMs.

In recent studies, we used neutron reflectometry to study the effect of ionic strength and film deposition techniques on the diffusivity of polyelectrolyte chains within linear PEMs.[27,28] In this work, we focus on *nl*PEMs and study the correlation between chain diffusivity, polyelectrolyte deposition time and film internal structure at different stages of film growth for films of varying deposition history.

Materials and Techniques

Branched polyethyleneimine (BPEI) with M_w=25 kDa and M_w/M_n = 2.50 was purchased from Aldrich. Hydrogenated polymethacrylic acid (*h*PMAA, or PMAA) with M_w 180 kDa and M_w/M_n=1.02 was purchased from Polymer Standard Services (PSS) GmbH, Germany. Deuterated poly(2-(dimethylamino)ethyl methacrylate) (*d*PDMAEMA, d15) with M_w 90 kDa and M_w/M_n 1.8, as well as deuterated PMAA (*d*PMAA) with molecular weight 180 kDa and M_w/M_n < 1.1 were purchased from Polymer Source, Inc. Hydrogenated 2-(dimethylamino)ethyl methacrylate monomer (DMAEMA), ethyl 2-bromoisobutyrate (EBiB), CuBr and 1,1,4,7,10,10-hexamethyltriethylenetetramine (HMTETA), hydrogenated and fully deuterated methyl sulfate (d6), as well as all solvents were purchased from Sigma-Aldrich. Ultrapure Milli-Q water (Millipore) with a resistivity of 18.2 MΩ/cm was used in all experiments. All other chemicals were purchased from Aldrich and used without further purification.

Polycation Synthesis and Characterization. Hydrogenated poly(2-(dimethylamino)ethyl methacrylate) (*h*PDMAEMA) homopolymer was synthesized by atom transfer radical polymerization (ATRP) as previously described.[29] In brief, DMAEMA (1.86 g), EBiB, CuBr and HMTETA were mixed in 8 mL of 2-propanol, at a molar ratio of 150:1:1:2, respectively. The

solution was stirred continuously in an argon atmosphere at room temperature for 12 h. The polymerization was terminated with liquid nitrogen and the solution diluted with THF. The copper salts were purified by passage through a basic aluminum oxide column. The polymer was precipitated in cold hexane and then dried in a vacuum oven at 25 °C overnight. Gel permeation chromatography (GPC) analysis of *h*PDMAEMA was performed in DMF with polystyrene (PS) standards. The M_w and M_w/M_n of the homopolymer were 90 kDa and 1.10, respectively, as determined by GPC. Quaternization of *h*PDMAEMA to obtain a 100% quaternized polycation with the molecular weight 95 kDa, abbreviated here as *h*QPC, was carried out at room temperature. To synthesize *h*QPC, *h*PDMAEMA was dissolved in a mixture of ethanol/benzene (v:v = 3:1), and a stoichiometric amount of hydrogenated dimethyl sulfate was added to the solution. The mixture was stirred at room temperature overnight. The precipitated product was washed with acetone three times and dried under vacuum overnight. A similar procedure was carried out to synthesize deuterated quaternized polycation (*d*QPC). To that end, *d*PDMAEMA was treated with fully deuterated rather than hydrogenated methyl sulfate. The degree of quaternization was determined by ^{1}H-NMR in D_2O at pH 9 as described elsewhere.[30] Briefly, after quaternization with dimethyl sulfate, a new peak at 3.3-3.4 ppm appeared, reflecting successful quaternization of the dimethylamino proton with a methyl group. The absence of a peak C at δ 2.3-2.5 ppm and a peak at δ 4.2-4.4 ppm, which both correspond to dimethylamino protons in *h*PDMAEMA, indicates complete quaternization of *h*PDMAEMA homopolymer (Figure S1).

Multilayer buildup and polyelectrolyte uptake experiments. LbL films were deposited on silicon wafer substrates (111, Institute of Electronic Materials Technology, Poland) by sequential dipping in 0.2 mg/mL PMAA and QPC solutions in 0.01 M phosphate/citrate buffer at pH 6.0 for 4, 8 or 24 min. Deposition time per each cycle during PEM assembly is denoted as a subscript. Prior to film deposition, silicon wafers were cleaned as described elsewhere[31] and primed with a monolayer of BPEI adsorbed from 0.2 mg/ml solution at pH 9 for 15 min. In between polymer deposition steps, the wafers were rinsed by immersing twice in 0.01 M phosphate/citrate buffer solutions at pH 6.0 for 2 min. The procedure was repeated until the required number of layers was reached.

For saturation experiments, which explored the maximum capacity of PEMs to absorb polyelectrolytes, silicon wafers with pre-deposited films of known thickness were exposed to 0.2

mg/mL PMAA or QPC solutions, and the amounts deposited within the films were monitored as a function of immersion time by measuring the ellipsometric thicknesses of the dry films. Films were removed from the solution, dried with a nitrogen flow and then the thickness was measured. The measurements continued until a constant film thickness was reached. The procedure was then repeated for each successive polyelectrolyte deposition step.

For saturation experiments *in situ,* a silicon wafer with a pre-deposited film of known dry thickness was placed into a liquid cell. The cell was then filled with 0.2 mg/mL PMAA or QPC solution. After an exposure time matching that of the films used in the dry measurements, the polyelectrolyte solution was replaced by a 0.01 M phosphate/citrate buffer solution at pH 6.0 and a thickness measurement was taken. The measurements were finalized after a constant wet thickness was reached by removing the sample from the cell, drying with nitrogen flow and measuring the dry thickness again.

For the penetration studies with NR, hydrogenated matrices consisting of 6-bilayer *h*PMAA/*h*QPC films (deposited using an 8-min per layer deposition time), were exposed to 0.2 mg/L solutions of *d*QPC in 0.01 M phosphate buffer at pH 6.0 for different time intervals. After rinsing with 18.2 MΩ/cm Milli-Q water and drying under nitrogen flow for 5 min, NR measurements were performed, and then the films were returned to the polymer solution for continued polymer uptake. Samples for internal structure studies were assembled using 4, 8 or 24 min deposition times per immersion cycle.

Spectroscopic Ellipsometry. Thicknesses and optical constants in both dry and swollen states of PEMs were characterized by a variable angle spectroscopic ellipsometer (VASE, M-2000 UV−visible−NIR [240−1700 nm] J. A. Woollam Co., Inc., Lincoln, NE, USA) equipped with a temperature-controlled liquid cell. For measurements in the liquid cell, the cell geometry dictated the angle of incidence to be 75°. In all experiments, the temperature was set to 25 °C. To avoid effects of absorption in the ultraviolet and near-infrared light region by the buffer solution, the working region of wavelength was set to 370.5 – 999 nm. Prior to deposition of PEM films, the thickness of oxide layer on the silicon substrate was measured. Dry measurements were carried out at three angles of incidence - 45°, 55°, and 65°.

To fit ellipsometric data obtained with dry films, a three-layer model was used, in which the first two layers represented the silicon substrate with silicon oxide, and the third layer represented the PEM film. The polymer layer was treated as a Cauchy material with a thickness

d, having a wavelength-dependent refractive index $n(\lambda) = A + B/\lambda^2 + C/\lambda^3$, where A, B and C are fitting coefficients, and λ is the wavelength. The film extinction coefficient was assumed to be negligible (k = 0). Thickness d and the three coefficients A, B and C were fitted simultaneously.

For *in situ* measurements, the thickness of dry films was first determined. Then, buffer or polyelectrolyte solutions were injected into a cell by a syringe in a sequence described in the multilayer buildup and exposure to polyion section. If polyelectrolytes were present in solutions, measurements were taken after rinsing the cell with 0.01 M phosphate buffer at pH 6.0 to avoid possible effects of the polyelectrolyte solution on the optical parameters of the system. To fit the ellipsometric data for the *in situ* measurements, a four layer model was used. An additional layer represents the semi-infinite buffer solution and was also treated as a transparent Cauchy medium, with a wavelength-dependent refractive index $n_{buf}(\lambda) = A_{buf} + B_{buf}/(\lambda)^2 + C_{buf}/(\lambda)^3$, where A_{buf}, B_{buf} and C_{buf} are fitting coefficients, and λ is the wavelength. For buffer solutions, A_{buf}, B_{buf} and C_{buf} were determined prior to *in situ* experiments by measuring $n_{buf}(\lambda)$ for a bare, clean silicon wafer installed in the liquid cell containing 0.01 M phosphate buffer at pH 6.0. After completion of the *in situ* measurements, the dry thicknesses of the films were measured again to assure that dry the thicknesses of the films used in swelling experiments were consistent with the independently measured dry film thicknesses obtained in the film growth experiments. In all experiments, the coefficients A, B, C were consistent within 5%.

Neutron Reflectometry. For neutron reflectometry, we used two designs of PEMs. The first design originally contained only hydrogenated polymers that were later penetrated by deuterated species. In fitting the NR data for this design, scattering densities for the hydrogenated base multilayer upon penetration of a deuterated PE from solution were held constant for all annealed samples, varying only the outermost layer's thickness, interfacial roughnesses, and *SLD*. The second design contained either a *d*PMAA or a *d*QPC block within the middle region of the film. Specifically, (*h*PMAA/*h*QPC)$_3$/(*d*PMAA/*h*QPC)/(*h*PMAA/*h*QPC)$_3$ and (*h*PMAA/*h*QPC)$_3$/(*h*PMAA/*d*QPC)/(*h*PMAA/*h*QPC)$_3$ architectures were deposited using 4, 8, 24 min deposition times.

Neutron reflectivity measurements were performed at the Spallation Neutron Source Liquids Reflectometer (SNS-LR) at the Oak Ridge National Laboratory (ORNL). The reflectivity data were collected using a sequence of 3.6-Å-wide continuous wavelength bands (selected from 2.63 Å < λ < 16.63 Å) and incident angles (ranging over 0.6° < θ < 2.34°). The

momentum transfer, $Q = (4\pi \sin\theta/\lambda)$, was varied over a range of $0.008\ Å^{-1} < Q < 0.193\ Å^{-1}$. Reflectivity curves were assembled by combining seven different wavelength and angle data sets together, maintaining a constant relative instrumental resolution of $\delta Q/Q = 0.023$ by varying the incident-beam apertures. Scattering densities within hydrogenated and deuterated stacks were averaged over the 12 constituent bilayers, each stack exhibiting its characteristic thickness, scattering density, and interlayer roughness. Those characteristic parameters were adjusted until the reflectivity curve was best fitted (minimized χ^2).

Results and Discussion

Film growth, swelling and polyelectrolyte ionization. Fig. 1 illustrates the effect of the deposition time on the growth of PMAA/QPC films. Fig 1A shows that the amount of material assembled within multilayer films increases with the deposition time, and switches from being constant per deposition cycle to being thickness-dependent when layer deposition time increases from 4 and 24 minutes. This effect is strong and results in a 5-fold difference in film thickness after ten deposition cycles using 4 or 24 minutes per layer. Qualitatively, this result is similar to observations by Schlenoff and co-workers, which were made for a different polyelectrolyte system studied at high salt concentrations,[31] where an almost two-fold increase in film thickness

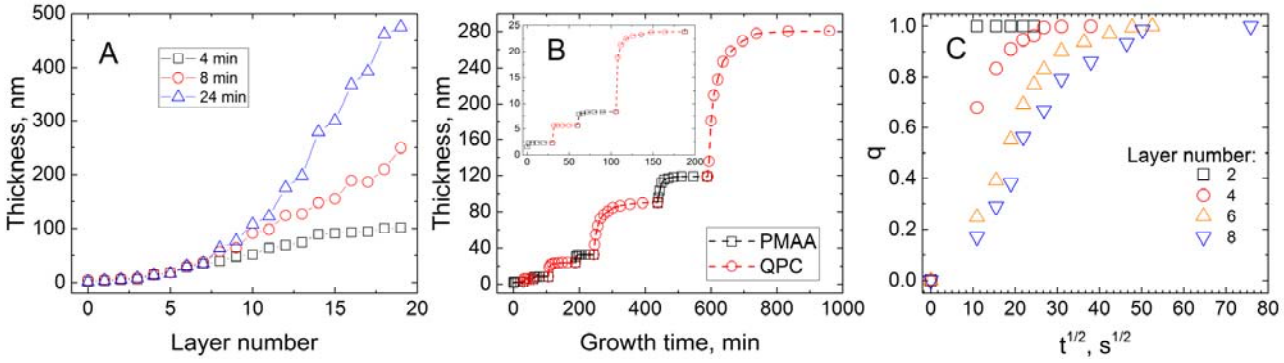

Fig. 1. (A) Thickness of dry PMAA/QPC films constructed using 0.1 mg/ml polymer solutions in 0.01 M phosphate buffer at pH 6 and 4, 8 or 24 min per-layer deposition times (squares, circles, and triangles, respectively). (B) Thicknesses of the dry PMAA/QPC film when the amount of polymer deposited was allowed to saturate at each deposition step. The inset presents an enlarged view of deposition within the first four layers. (C) The kinetics of QPC uptake by 1-, 3-, 5- and 7-layer films containing PMAA as the top layer (2nd, 4th, 6th and 8th layer deposition steps).

was reported when the polyelectrolyte deposition time increased from 8 to 20 min. Fig. 1B shows the growth of the film when the deposition time per layer was not fixed, but instead the mass of the deposited polymers was allowed to equilibrate and reach a plateau value at each deposition step. Twice as much QPC as PMAA was deposited, in agreement with the higher molecular weight of the QPC repeat units compared to PMAA (150 and 72 g/mol, respectively).

Importantly, both the masses of PMAA and QPC deposited at each film growth step and the kinetics of polyelectrolyte uptake were strikingly different between the first several layers and subsequent film deposition steps (Fig. 1B). The small mass deposited within the first layers (2-4 mg/m^2, calculated assuming a density of dry LbL films of 1 g/cm^3) is consistent with a monolayer coverage, indicating binding of polyelectrolytes only in the outermost film region. In contrast, during adsorption of the film's 8th layer, QPC mass uptake was as large as ~160 mg/m^2, suggesting deposition of QPC within the interior of the film. Deposition of polyelectrolytes at the film surface or within the interior was kinetically distinct (Fig. 1B and C). While adsorption of polyelectrolytes within the first and second layers (PMAA and QPC, respectively) saturated within the first 2 minutes, equilibration of the QPC mass deposited within the 8th layer of the film with an initial thickness of 120 nm continued for as long as 150 min. Rapid binding of polyelectrolytes within the first layers was limited by the diffusion flux from solution and persisted as the mode of polyelectrolyte adsorption till the 4th layer (Fig. 1C). A similar trend was observed for uptake of PMAA (Fig. S2). For films with a larger number of layers, fast polyelectrolyte binding and saturation at the film's surface was followed by the slow diffusion of a large amount of material within the film interior. Figure 1C highlights these differences by showing the kinetics of QPC uptake by the film plotted as a function of the normalized polymer mass uptake, q versus $\sqrt{t}$, where q is a normalized mass uptake, calculated from the dry film thickness as $(l_t - l_0)/(l_\infty - l_0)$, where l_0, l_t, l_∞ – initial, effective (at time t) and equilibrated thicknesses of the dry films, and t denotes the exposure time.[32] The maximum film thickness at which polyelectrolytes adsorbed at the film surface rather than penetrating into the interior (corresponding to a three-layer film, Figs. 1B and C) was about 8 nm. After subtraction of the thickness of the precursor BPEI layer of 1.5 nm, the remaining 6.5 nm can be taken as an estimate of a dense, near-substrate zone in which chains are immobilized as a result of adsorption and pinning to a solid surface and hence are inhibited from rearranging and allowing penetration of newly binding chains.

While the data in Fig. 1 are presented for dry films, dynamic interpolymer binding and uptake of polyelectrolytes within the film bulk are expected to cause significant film swelling. Fig. 2A shows changes in the degree of swelling as PMAA/QPC film was built up when saturated with polyelectrolytes at each deposition step. The swelling ratio was determined as the ratio of wet film thickness, measured by *in situ* ellipsometry in the presence of buffer above the growing film, to the thickness of the dry films. For measurements of wet film thicknesses, polyelectrolyte solutions were replaced with a buffer at desired time points in order to inhibit the uptake of polyelectrolytes within the film and avoid the interference of an increased refractive index of the backing solutions. For measurements of dry film thicknesses, films were taken out of the polyelectrolyte solutions, repeatedly rinsed with 0.01 M phosphate buffer and dried in a nitrogen flow. The swelling data correlate well with the uptake of polyelectrolytes within the films. While films composed of up to three polyelectrolyte layers contained less than 100% of water (calculated by deriving water fraction from the swelling thickness, assuming a constant density), consecutive film construction steps caused a dramatically larger uptake of water, and the swelling ratio oscillated between the limiting values of 3.8 and 2.4 for deposition of QPC and PMAA, respectively. Based on these ratios, *nl*PEMs swell much more than linear PEMs, whose water content is usually about 40-60%.[33-35] The inset in Fig. 2B also shows the correlation between the polyelectrolyte mass deposited and film swelling. Note that the data for film swelling as a function of QPC deposited within the 6th and 8th deposition cycles collapses onto almost the same curve when plotted as a function of the relative amount of QPC bound to the film (the ratio of the mass of QPC to the initial mass of the film at the beginning of polycation deposition), again suggesting penetration of QPC throughout the entire film. The uptake of QPC (which carries permanent charge) results in a strong increase in film swelling, caused by the excess charge brought in by QPC charged loops, *i.e*. QPC units that do not participate in formation of ionic pairs with PMAA. The addition of a weak polyelectrolyte – PMAA – on the contrary, resulted in film de-swelling as charge in the PMAA loops was suppressed as larger amounts of the polyacid accommodated within the film.[36] As polyelectrolytes were allowed enough time to diffuse through the entire film, the limiting swelling ratios oscillated between those characteristic of QPC and of PMAA, depending on which was being added.

To quantitatively assess diffusion of the polyelectrolyte with a permanent charge, QPC, within the film, we used a Fickian diffusion model. The diffusion coefficients for QPC chains

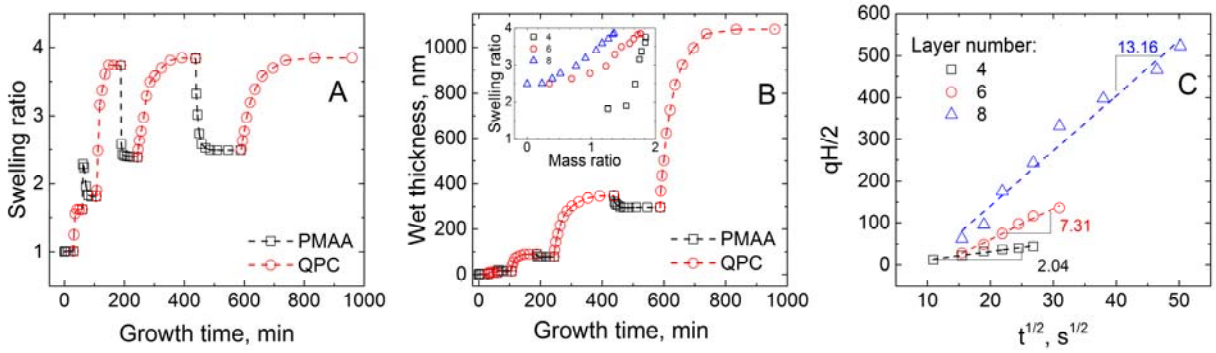

Fig. 2. (A) The swelling ratio of a PMAA/QPC film monitored during deposition of the first 8 layers. Red circles and black squares correspond to exposure of the film to QPC and PMAA solutions, respectively. (B) *in situ* thicknesses of PMAA/QPC film when deposited polymer amounts were allowed to saturate at each deposition step. (C) qH/2 versus $t^{1/2}$ dependence plotted for the construction of 4th, 6th and 8th layers of the QPC/PMAA film.

can be determined from the slopes of the initial linear region of $q^2H^2/4$ plotted against time (Fig. 2C) following the equation $Dt = \frac{q^2H^2}{4}$, where D is the diffusion coefficient, q is the normalized mass uptake, calculated from measurements of dry film thicknesses as $(l_t - l_0)/(l_\infty - l_0)$, where l_0, l_t, l_∞ – initial, effective (at time t) and equilibrium thicknesses of dry films, t – exposure time to a polyelectrolyte solution, and H − film thickness at time t. In this simplistic model, the choice of film thickness presents the biggest uncertainty.[37] We have chosen H to be the wet film thickness as measured with spectroscopic ellipsometry. The value of H increases with time with the uptake of polymer chains. While a reliable determination of the diffusion constant was not feasible based on our data when chains diffused in solution and bound to the film surface (the deposition of the 2nd layer), diffusion coefficients determined from the slopes in Fig. 2C for layer numbers 4, 6 and 8 reflected penetration of QPC chains into the multilayer film. The diffusion coefficients for transport of QPC chains within the film were $1.3\pm0.5\times10^{-13}$ cm^2/s, $1.7\pm0.8\times10^{-12}$ cm^2/s and $5.4\pm1.2\times10^{-12}$ cm^2/s for deposition of the 4th, 6th and 8th layers, respectively, *i.e.* values of D increased with a lower rate as the films grew thicker, indicating 'fading' memory of the attachment to the hard substrate. These values are five orders of magnitude smaller than those

found for diffusion of free polyelectrolyte chains of similar molecular weight in solution[22,38], and similar to those observed for the mobility of QPC chains within linearly deposited LbL films in the presence of high concentrations of salts.[37]

As for the mechanism of polyelectrolyte diffusion, it is likely that QPC diffuses within the films while remaining bound to PMAA chains rather than in its "free" state (diffusion of "free" polyelectrolyte chains was earlier found in a different LbL system composed of natural macromolecules and/or synthetic polypeptides[39]). In the PMAA/QPC system, while chains remain bound to the film matrix during polymer uptake from solution, propagation of the invading chains within the bulk of the film is likely to occur though the exchange of polyelectrolyte 'sticky' binding points in the electrostatic network. The large number of invading QPC chains diffusing within the film introduce a large charge excess that is accommodated by loops of polymer chains bound within a network of electrostatically associated chains (Scheme 1). The multilayer is reminiscent of surface-immobilized non-stoichiometric polyelectrolyte complexes, which are significantly swollen by excess charge accumulated in polymer loops and the osmotic pressure originating from the inclusion of charge-compensating small counter-ions.

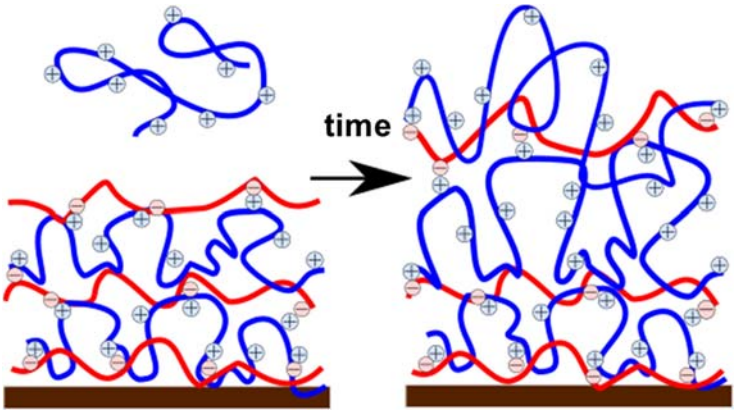

Scheme 1. Formation of non-linear polyelectrolyte multilayers.

As shown in Fig. 2, binding a weak polyelectrolyte (PMAA) rather than QPC has an opposite effect on film swelling, *i.e.* the film deswelled as more polyelectrolyte was bound. We hypothesize that this is due to the adjustment of charge in the PMAA chains to the total charge in the *nl*PEM film, and have directly detected charge renormalization using FTIR spectroscopy. While in earlier studies, this technique was used by several groups, including ours, to study

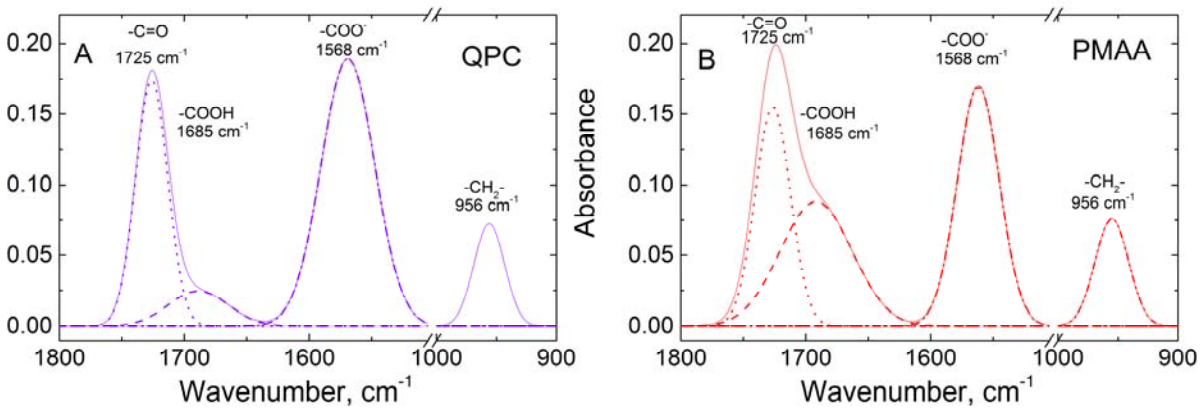

Fig. 3. FTIR spectra of dry PMAA/QPC films containing either QPC (A, 10-layer film) or PMAA (B, 11-layer film) as and outermost layer. The data illustrate reduced ionization of PMAA in the films containing PMAA as the outermost layer.

ionization of weak polyelectrolytes assembled within linear PEMs,[36,40] here we apply FTIR spectroscopy to study the ionization of PMAA within *nl*PEMs. Fig. 3 shows FTIR spectra of a 10-layer PMAA/QPC film deposited in saturation conditions and terminated with QPC, as well as the same film after deposition of PMAA as the 11th layer in the film. Both spectra show vibrational bands at 1725 cm^{-1} and 1568 cm^{-1} associated with stretching vibrations of uncharged carboxylic groups (ν, −C═O) and asymmetric stretching vibrations of the carboxylate groups (ν_{as}, −COO$^-$), respectively, as well as a small peak at 1685 cm^{-1} associated with hydrogen-bonded dimers (−COOH) of protonated carboxylic groups. The ionization degree of PMAA within the assembled multilayers was calculated as the ratio of the area of −COO$^-$ to the sum of −COOH and −COO$^-$ absorbances, assuming equal extinction coefficients for vibrations associated with these bands.[41] This quantification gave the ionization degrees of PMAA as 60±2% and 38±2% for films terminated with QPC and PMAA, respectively. These data clearly show that uptake of QPC causes an increase in the average ionization of assembled PMAA chains due to formation of ion pairs between QPC and previously uncharged PMAA units, while the addition of PMAA causes suppression of the ionization of PMAA in the adsorbed polymer loops, likely as a result of accumulation of an excess of negative charge within the film. Also note that the integrated intensity of the 956 cm^{-1} band characteristic of QPC and probably associated with CH_2 wagging vibrations of methylene group,[42] remained unchanged after PMAA

addition (Fig. 3), suggesting that polyacid binds to the electrostatically associated network without causing desorption of QPC chains.

Film internal structure: neutron reflectometry studies. In earlier studies, neutron reflectometry has been applied to establish correlations between the strength of intermolecular binding and

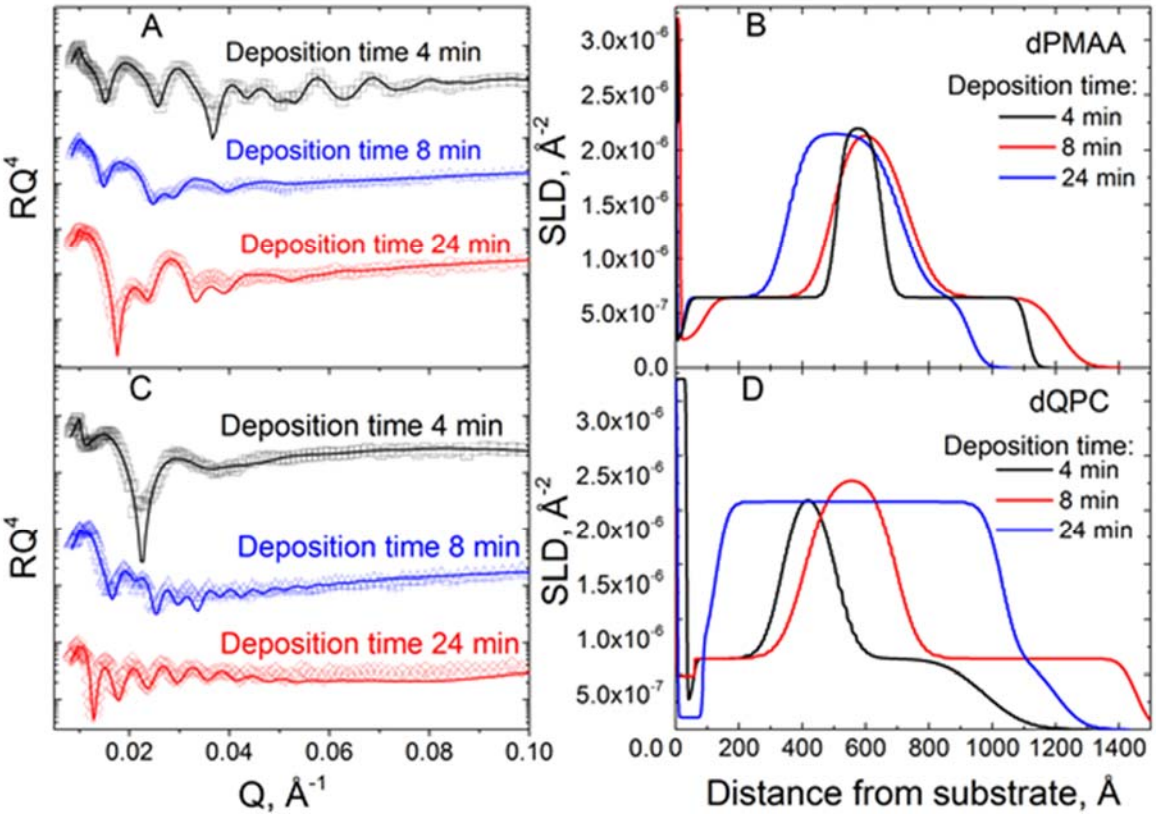

Fig. 4. Reflectometry data (A, C) and scattering length density profiles for QPC/PMAA films formed using hydrogenated and deuterated components. (B) SLD profiles of films assembled using *d*PMAA as a marker layer with design (*h*PMAA/*h*QPC)$_x$ / (*d*PMAA/*h*QPC) / (*h*PMAA/ *h*QPC)$_y$ using 4, 8 and 24 min deposition times (black, red and blue lines, respectively) where x and y indicate the number of bilayers (for 4 and 8 min deposition times x and y were 4; for the 24 min deposition time, x and y are 3 and 2 respectively. (D) SLD profiles of films assembled using *d*QPC as a marker layer with design (*h*PMAA/*h*QPC)$_x$ / (*h*PMAA/*d*QPC) / (*h*PMAA /*h*QPC)$_y$ for samples with 4, 8 and 24 min deposition times (black, red and blue lines, respectively) where x and y reflect the number of bilayers (for 4 and 8 min deposition times x and y were 4; for the 24 min deposition time x and y are 3 and 2, respectively).

film intermixing for linear PEMs of electrostatically assembled films, [22,27,30,43,44,] and films stabilized by hydrogen bonding.[45] In this work, neutron reflectometry is used to study the effect of a new parameter important for *nl*PEMs– layer deposition time – on internal film structure and to quantitatively measure the diffusion of invading polyelectrolytes into the film.

To that end, we have designed two different types of experiments. In the first scenario (Design I), films were constructed in which deuterated polyelectrolytes (either *d*PMAA or *d*QPC) were included as 'marker' layers in the middle of PEMs constructed using hydrogenated

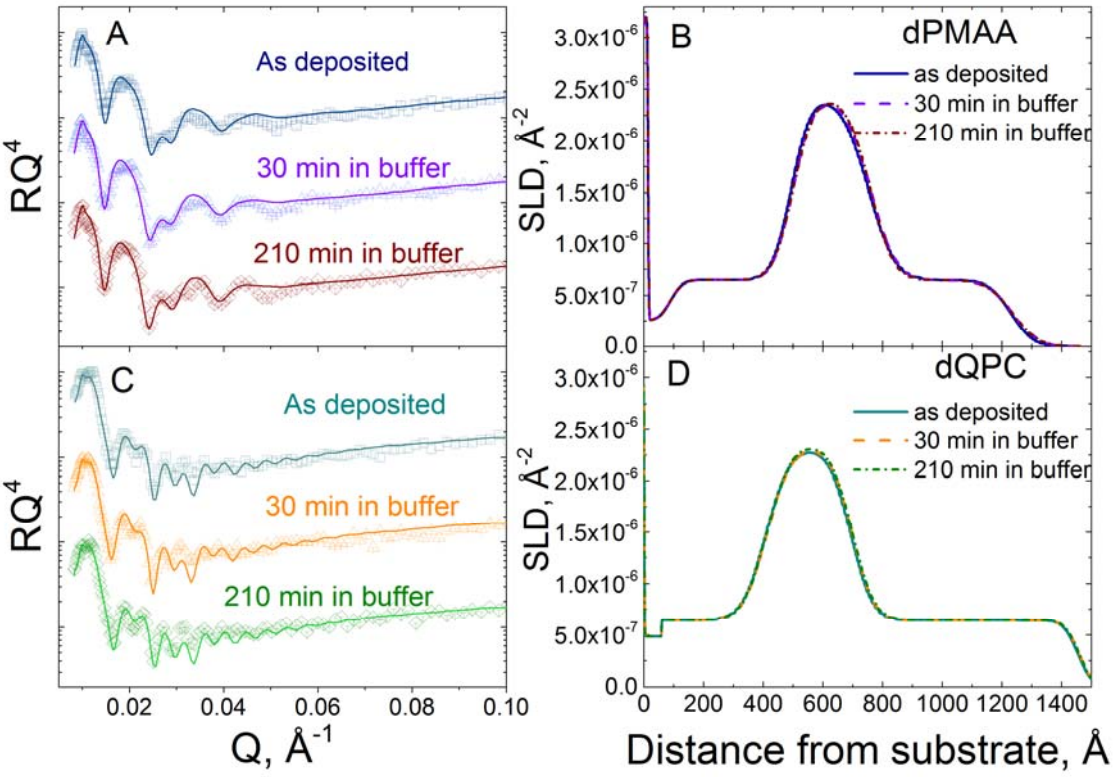

Fig. 5. Reflectometry data (A, C) and scattering length density profiles (B, D) for PMAA/QPC films formed using hydrogenated and deuterated components. (B) Film assembled using *d*PMAA as a marker layer with design (*h*PMAA/*h*QPC)$_4$ / (*d*PMAA/*h*QPC) / (*h*PMAA/*h*QPC)$_4$ prepared using an 8 min deposition time after 30 and 210 min exposure to 0.01 M phosphate buffer at pH 6.0. (D) Film assembled using *d*PMAA as a marker layer with design (*h*PMAA /*h*QPC)$_4$ / (*h*PMAA/*d*QPC) / (*h*PMAA/*h*QPC)$_4$ using an 8 min deposition time after 30 and 210 min exposure to 0.01 M phosphate buffer at pH 6.0.

polymers, wherein each layer was assembled using a specific deposition time (Figs. 4 and 5). In the second scenario (Design II, shown below in Fig. 6), films were first constructed using hydrogenated polymers, and then the kinetics of penetration of deuterated QPC chains into the film was studied as a function of exposure time to a *d*QPC solution. The reflectivity model for Design I consisted of the BPEI priming layer and three hydrogenated/deuterated/hydrogenated stacks. The *SLD* of the hydrogenated stacks was constrained to the value for the hydrogenated matrix determined in an independent measurement of hydrogenated films. The *SLD* of the deuterated block was found by fitting the reflectivity data. The model for Design II initially consisted of only two stacks – a priming layer and a hydrogenated matrix. Upon absorption of deuterated chains, an additional stack representing the hydrogenated matrix enriched with deuterated polymers was introduced into the model.

Fig. 4 shows neutron reflectivity data and the calculated *SLD* profiles of *nl*PEMs constructed using per-layer deposition times which were constant for each individual film, but varied between different *nl*PEMs. Because the amount of material deposited was strongly time-dependent and, due to instrumental resolution, the total film thickness in NR should not exceed

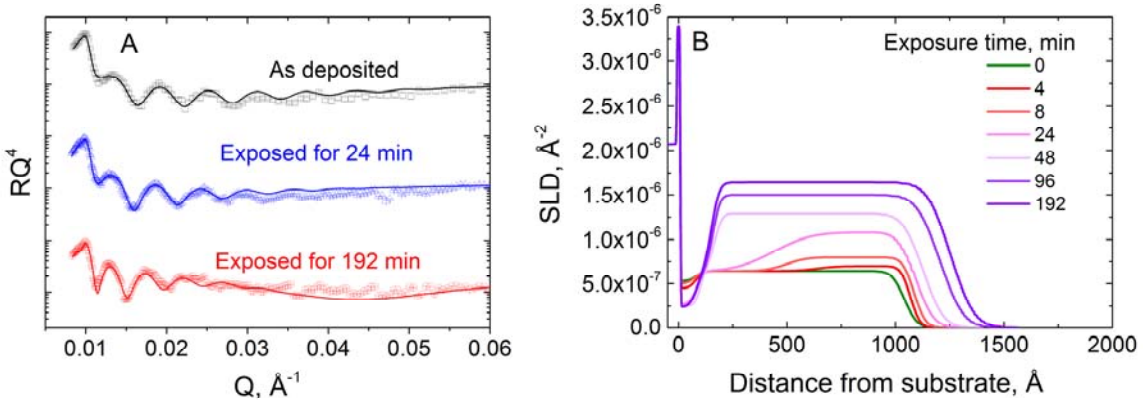

Fig. 6. The effect on the film internal structure of the exposure of a 6-bilayer hydrogenated PMAA/QPC film to a 0.2 mg/ml *d*QPC solution, as illustrated by neutron reflectometry data (plotted as RQ^4 to enhance small features) (left) and the corresponding fitted scattering length density profiles (right).

~350 nm,[1] films constructed using longer deposition times by design had fewer polyelectrolyte layers. Fig. 4 shows the dramatic effect of layer deposition time on internal film structure. Films constructed using 4, 8, and 24 min deposition times demonstrated increasingly larger and more diffuse deuterated stacks. For 4-min, 8-min-and 24-min film assemblies, the integrated area under the stacks of *d*PMAA and *d*QPC increased as 1 : 1.8 : 2 and 1 :1.7 : 3.4, respectively. This is in agreement with an increase of the total mass of polymers bound within *nl*PEM films for different deposition times. This ratio, derived from ellipsometric data, yields values of 1 : 1.7 : 2.6 and 1 : 1.8 : 2.5 for films of comparable thickness (Fig. 1A).

Tracking the increase in deposited polymer mass, the interfacial full width, σ_{int}, between hydrogenated and deuterated blocks increased from 6.7 to 12.0 nm for *d*PMAA, indicating greater intermixing between hydrogenated and deuterated stacks. Interestingly, the maximum SLD of *d*PMAA and *d*QP is independent of the layer deposition time, indicating there is a constant ratio between hydrogenated and deuterated chains as they mix within the multilayer (Tables S1-S6). At the same time, the kinetics of the increase in the deuterated stack width was strikingly different for *d*PMAA- and *d*QP-containing films (Fig. 4). An increase in either the width or the integrated SLD of the deuterated stacks indicates both an increased spreading and a larger amount of deuterated polymer adsorbed at each deposition step. Diffusion of polymer already within the films is coupled with the diffusion of arriving polyelectrolyte chains into the multilayer matrix, and so more polymer can be bound at the film surface from solution as deposition progresses. Therefore, the amount of additional adsorbed material is limited by the interdiffusion/penetration rate of polyelectrolyte into the existing film. The faster intermixing of QPC into the film and the larger amount of QPC adsorbed within each layer compared to *d*PMAA can be explained by the different degrees of polymerization (DP) of PMAA and QPC (DPs 2090 and 570 for PMAA and QPC, respectively), which leads to more sluggish dynamics of PMAA chains in the film. Diffusion coefficients for *d*PMAA and *d*QPC penetration estimated from d^2 vs. t dependences using the data in Table 1 yield estimated values of 3.9×10^{-15} cm^2/s and 3.5×10^{-14} cm^2/s, respectively. These values, estimated from measurements of dry *nl*PEMs, are two orders of magnitude lower than those measured for the intrusion of polyelectrolyte

[1] Upstream collimation determines the angular divergence of the incident beam ($\delta\theta$) which, in turn, is the dominant term in the instrumental resolution of the Liquids Reflectometer ($\delta Q/Q = \delta\theta/\theta$, where θ is the angle of incidence onto the sample). The maximum resolvable film thickness is given by $d_{max}= 2\pi/\delta Q$, which is about 350 nm for these measurements.

Table 1. Fitted parameters of the thickness and interfacial roughness of a deuterated stack incorporated within the hydrogenated matrix of different PMAA/QPC films (Design I).

	*d*PMAA stack		*d*QPC stack	
Deposition time, min	d, nm	σ_{int}, nm	d, nm	σ_{int}, nm
4	14.4	6.7	16.7	12.8
8	26.0	12.0	26.7	15.8
24	35.2	12.0	90.6	16.0

molecules into wet films. Penetration of polyelectrolyte chains into the films is also determined by the presence of a 'supply' of polyelectrolyte chains in solution and did not occur when films were immersed in polyelectrolyte-free buffer solutions. Fig. 5 shows that *nl*PEMs, featuring deuterated marker layers in the middle region of the film, using 8 min deposition time did not show any changes in internal structure upon exposure to a 0.01 M phosphate buffer solution for as long as two hours (Tables S7-S10).

We next aimed to directly observe the diffusion of deuterated polyelectrolyte chains *as they* invade the film. In this experiment, a hydrogenated 6-bilayer *nl*PEM assembled using the 8-min per layer protocol containing PMAA as the outermost layer was immersed in a 0.2 mg/ml solution of *d*QPC; the film was taken out of solution, rinsed with buffer and dried prior to the NR measurement. Fig. 6 summarizes the NR data for various times of exposure to *d*QPC solutions (Tables S11-S17). Upon exposure to the deuterated polymer solution, the oscillation minima shift to lower *Q* values indicating an increase in total film thickness. The reflectivity data for the initially hydrogenated matrix have been fitted using a precursor film plus a single stack. After exposure to the deuterated polymer, we use a two-stack model, with the bottom stack corresponding to the hydrogenated material, and the upper stack associated with the addition of deuterated polymer. The fitted neutron reflectometry profiles are shown in Fig. 6, right. The addition of *d*QPC to the film is observed from an increase in *SLD* values, which at shorter times occurred only within the upper part of the film. As exposure time increased, an enhanced *SLD* zone propagated deeper in the film until the deposited polymer was distributed throughout the film. A zone impermeable to *d*QPC penetration even at longer times is seen in the fitted *SLD* profiles in Fig. 6. The total thickness of this zone of hydrogenated polyelectrolytes (Table S16) was ~150 Å, which included a 75-Å layer of lower *SLD* incorporating the BPEI layer. The

remaining 75 Å of the PMAA/QPC film, approximately corresponding to a single bilayer, is strongly bound to the substrate and cannot be replaced by deuterated chains. This is in good agreement with the 6.5 nm thickness of the dense near-substrate zone estimated from ellipsometry experiments (see above). Fig. 7A shows the kinetics of *d*QPC penetration into the film as represented by changes in the width of the deuterated stack *d*. The diffusion coefficient was determined to be $1.1\pm0.1\times10^{-14}$ cm^2/s from the d^2 *vs*. *t* graph shown as an inset in Fig. 7A. This value is one to two orders of magnitude smaller than that of QPC chains determined using the thicknesses of swollen films in Fig. 2, since the diffusion coefficient will be underestimated if the diffusion distances are taken from dry film measurements. Fig. 7B shows the plateau

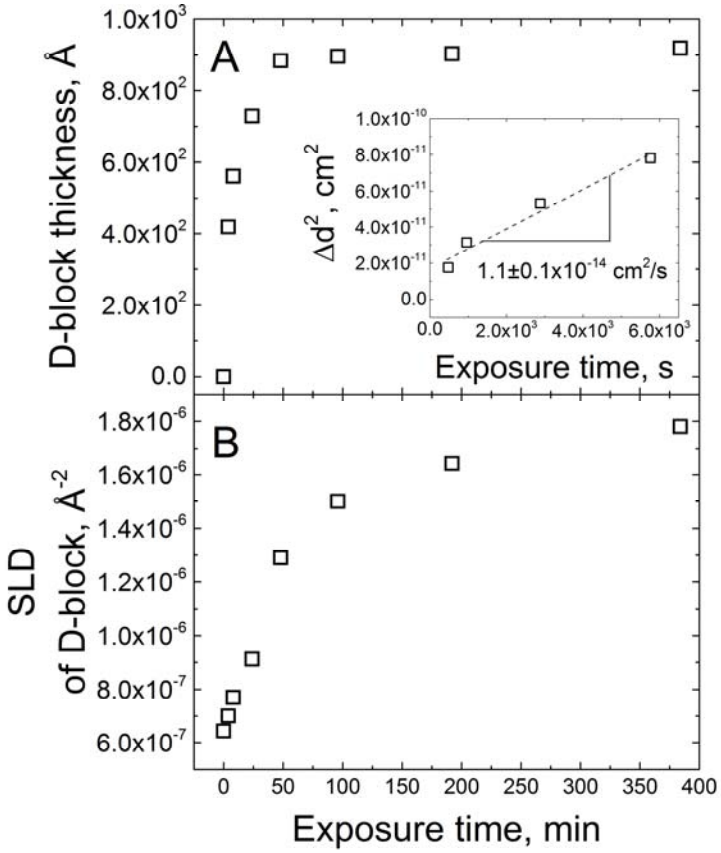

Fig. 7. Time dependence of the polyelectrolyte penetration depth, *d* (A) and the plateau SLD value (B) during the invasion of *d*QPC chains into a hydrogenated 6-bilayer PMAA/QPC film assembled using the 8 minutes per layer deposition procedure.

values of *SLD* of *d*QPC-containing films, which are largely composed of hydrogenated PMAA and deuterated QPC chains, as a function of time. By comparing the data in Figs. 7A and B, two regimes for *d*QPC penetration into *nl*PEM can be distinguished. The first regime is caused by diffusion of the initial *d*QPC, which occurs with the diffusion coefficient estimated above. The second process involves a slower enrichment of PMAA/QPC complexes with deuterated chains. This slower addition of deuterated chains is rate limited by the sluggish chain rearrangements of earlier formed *h*PMAA/QPC contacts to accommodate excess *d*QPC within the film. The arriving polyelectrolyte chains bring in excess charge that causes the film to swell as shown in Fig. 2 above.

The fitted plateau values of *SLD* also enable us to estimate the relative amounts of hydrogenated and deuterated polymers, as well as the content of water in the LbL film. We first analyzed the initial, as deposited PEM which contained only hydrogenated polyelectrolytes. The total SLD_{H} of this matrix was found by fitting the reflectivity data to be 6.43×10^{-7} Å^{-2}. One can express the total SLD_{H} of the hydrogenated matrix as follows:

$$SLD_{\mathrm{H}} = \omega_{h\mathrm{PMAA}} SLD_{h\mathrm{PMAA}} + \omega_{h\mathrm{QPC}} SLD_{h\mathrm{QPC}} + \omega_{\mathrm{H_2O}} SLD_{\mathrm{H_2O}}, \qquad (1)$$

where the ω values represent the mass fractions of the different film components. *SLD* values of

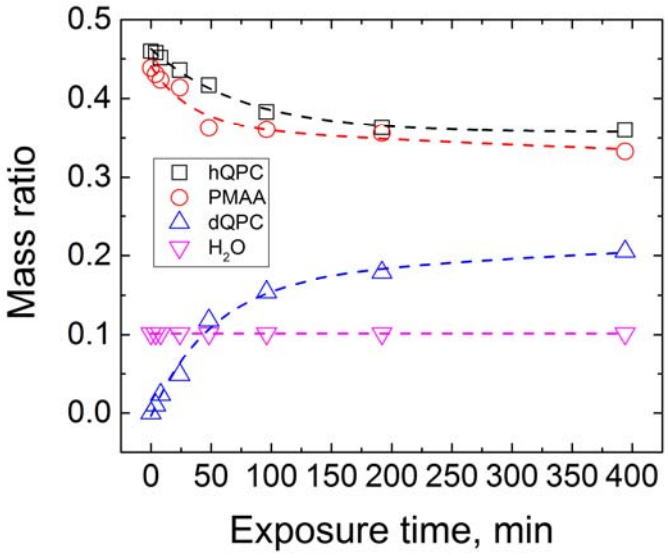

Fig. 8. The effect of the exposure time of a hydrogenated QPC/PMAA film to a 0.2 mg/ml dQPC solution on the mass ratios of all components within the 6-bilayer *nl*PEM film.

each component were calculated using known atomic densities and polymer atomic compositions (Table S18). The values of ω were fitted simultaneously with the boundary conditions set for ω for PMAA and QPC not to exceed 0.6, and for ω for H_2O not to exceed 0.2, and the sum of the ω components adds up to 1. Only one solution for film composition was found, i.e. $\omega_{h\mathrm{QPC}} = 0.46$, $\omega_{h\mathrm{PMAA}} = 0.439$ and $\omega_{\mathrm{H2O}} = 0.101$. The water content of 10.1% is in a good agreement with previously reported values found using neutron reflectometry for linear PEMs.[46]

The fitted values of $\omega_{h\mathrm{QPC}}$ and $\omega_{h\mathrm{PMAA}}$ were taken as initial values for further calculations, performed for films after the addition of *d*QPC. The water content in the films was assumed to be constant for all film compositions, because samples were dried with the same procedure. Also, the amount of deuterated polyelectrolyte was allowed to increase assuming no loss of hydrogenated polymer. Then, after exposure of the film to *d*QPC, the *SLD* of the top block can be calculated as follows:

$$SLD_{\mathrm{D}} = \omega_{h\mathrm{PMAA}} SLD_{h\mathrm{PMAA}A} + \omega_{h\mathrm{QPC}} SLD_{h\mathrm{QPC}} + \omega_{\mathrm{H_2O}} SLD_{\mathrm{H_2O}} + \omega_{d\mathrm{QPC}} SLD_{d\mathrm{QPC}} \qquad (2)$$

where two additional parameters, *i.e.* $\omega_{d\mathrm{QPC}}$ and the *SLD* of *d*QPC, with $\omega_{d\mathrm{QPC}}$ set to be less than $\omega_{h\mathrm{QPC}}$. With the fitted values of the parameters set to be less than initial values of the hydrogenated matrix, the equation was fitted to find $\omega_{d\mathrm{QPC}}$. The calculated mass ratios (ω) of each component in the stack enriched with the deuterated material are provided in Table S19. The calculations indicate that the content of *d*QPC in the film increases from zero to ~20% with time, while the fractional content of hydrogenated PMAA and QPC decreases to below 40% of the total mass. These results show that even after long-term (192 min) exposure of *nl*PEMs to *d*QPC, films contain both hydrogenated and deuterated polycation chains, *i.e.* enrichment with polycations is likely to occur as co-adsorption of additional *d*QPC chains rather than *via* replacement of the original *h*QPC.

Conclusion

This work presents quantitative studies of dynamic polyelectrolyte multilayers that exhibit non-linear growth. The growth of electrostatically assembled films is strongly time-dependent, with the amount of material deposited at each deposition step increasing with the number of deposition steps. Diffusion of polyelectrolytes during film deposition was directly correlated with this thickness increase, and diffusion coefficients of the penetrating polymer chains were estimated from ellipsometry and neutron reflectometry measurements. While

diffusion coefficients of polyelectrolyte chains were drastically slower than in solution for both dry and solvent-swollen films, chain diffusion occurs within *nl*PEMs, which remain highly swollen. Swelling of the film is related to penetration of polyelectrolyte with excess charge throughout the entire film thickness, and the binding of permanently charged and weak polyelectrolytes can have opposite effects on film swelling, resulting in periodic oscillations of film swelling with layer number. Furthermore, deposition time can be used to control the internal structure of *nl*PEMs as shown by neutron reflectometry, and polyelectrolyte layers can be localized within the film by reducing the deposition time allowed for layer assembly. The estimated values of diffusion coefficients argue for diffusion of polyelectrolytes within the film in their bound rather than "free" state.

Supporting Information

The fitting parameters of neutron reflectivity, *SLD*s, raw data and diffusion coefficients. This material is available free of charge via the Internet at http://pubs.acs.org.

Corresponding Author

*E-mail: svetlana@tamu.edu.

Notes

The authors declare no competing financial interest.

Acknowledgment

We thank Michael Rubinstein (University of North Carolina at Chapel Hill) for helpful discussions. This work was supported by the National Science Foundation under Award DMR-1610725 (S.S.). Neutron measurements were performed at the Spallation Neutron Source at the Oak Ridge National Laboratory, managed by UT-Battelle, LLC, for the DOE under contract No. DE-AC05-00OR22725.

References

(1) Decher, G.: Layer-by-Layer Assembly (Putting Molecules to Work). In *Multilayer Thin Films*; Wiley-VCH Verlag GmbH & Co. KGaA, 2012; pp 1-21.

(2) Pavlukhina, S.; Sukhishvili, S. Polymer assemblies for controlled delivery of bioactive molecules from surfaces. *Advanced Drug Delivery Reviews* **2011**, *63*, 822-836.

(3) Liu, X.; Han, F.; Zhao, P.; Lin, C.; Wen, X.; Ye, X. Layer-by-layer self-assembled multilayers on PEEK implants improve osseointegration in an osteoporosis rabbit model. *Nanomedicine: Nanotechnology, Biology and Medicine* **2017**, *13*, 1423-1433.

(4) Min, J.; Choi, K. Y.; Dreaden, E. C.; Padera, R. F.; Braatz, R. D.; Spector, M.; Hammond, P. T. Designer Dual Therapy Nanolayered Implant Coatings Eradicate Biofilms and Accelerate Bone Tissue Repair. *ACS Nano* **2016**, *10*, 4441-4450.

(5) Hsu, B. B.; Hagerman, S. R.; Hammond, P. T. Rapid and efficient sprayed multilayer films for controlled drug delivery. *Journal of Applied Polymer Science* **2016**, *133*, n/a-n/a.

(6) Lavalle, P.; Gergely, C.; Cuisinier, F. J. G.; Decher, G.; Schaaf, P.; Voegel, J. C.; Picart, C. Comparison of the Structure of Polyelectrolyte Multilayer Films Exhibiting a Linear and an Exponential Growth Regime: An in Situ Atomic Force Microscopy Study. *Macromolecules* **2002**, *35*, 4458-4465.

(7) Schoeler, B.; Kumaraswamy, G.; Caruso, F. Investigation of the Influence of Polyelectrolyte Charge Density on the Growth of Multilayer Thin Films Prepared by the Layer-by-Layer Technique. *Macromolecules* **2002**, *35*, 889-897.

(8) Ramsden, J. J.; Lvov, Y. M.; Decher, G. Determination of optical constants of molecular films assembled via alternate polyion adsorption. *Thin Solid Films* **1995**, *254*, 246-251.

(9) Elbert, D. L.; Herbert, C. B.; Hubbell, J. A. Thin Polymer Layers Formed by Polyelectrolyte Multilayer Techniques on Biological Surfaces. *Langmuir* **1999**, *15*, 5355-5362.

(10) Ruths, J.; Essler, F.; Decher, G.; Riegler, H. Polyelectrolytes I: Polyanion/Polycation Multilayers at the Air/Monolayer/Water Interface as Elements for Quantitative Polymer Adsorption Studies and Preparation of Hetero-superlattices on Solid Surfaces. *Langmuir* **2000**, *16*, 8871-8878.

(11) Picart, C.; Lavalle, P.; Hubert, P.; Cuisinier, F. J. G.; Decher, G.; Schaaf, P.; Voegel, J. C. Buildup Mechanism for Poly(l-lysine)/Hyaluronic Acid Films onto a Solid Surface. *Langmuir* **2001**, *17*, 7414-7424.

(12) Picart, C.; Mutterer, J.; Richert, L.; Luo, Y.; Prestwich, G. D.; Schaaf, P.; Voegel, J. C.; Lavalle, P. Molecular basis for the explanation of the exponential growth of polyelectrolyte multilayers. *Proceedings of the National Academy of Sciences of the United States of America* **2002**, *99*, 12531-12535.

(13) Richert, L.; Lavalle, P.; Payan, E.; Shu, X. Z.; Prestwich, G. D.; Stoltz, J.-F.; Schaaf, P.; Voegel, J.-C.; Picart, C. Layer by Layer Buildup of Polysaccharide Films: Physical Chemistry and Cellular Adhesion Aspects. *Langmuir* **2004**, *20*, 448-458.

(14) Yang, Y.-H.; Malek, F. A.; Grunlan, J. C. Influence of Deposition Time on Layer-by-Layer Growth of Clay-Based Thin Films. *Industrial & Engineering Chemistry Research* **2010**, *49*, 8501-8509.

(15) Wu, B.; Li, C.; Yang, H.; Liu, G.; Zhang, G. Formation of Polyelectrolyte Multilayers by Flexible and Semiflexible Chains. *The Journal of Physical Chemistry B* **2012**, *116*, 3106-3114.

(16) Liu, G.; Zou, S.; Fu, L.; Zhang, G. Roles of Chain Conformation and Interpenetration in the Growth of a Polyelectrolyte Multilayer. *The Journal of Physical Chemistry B* **2008**, *112*, 4167-4171.

(17) Wong, J. E.; Zastrow, H.; Jaeger, W.; von Klitzing, R. Specific Ion versus Electrostatic Effects on the Construction of Polyelectrolyte Multilayers. *Langmuir* **2009**, *25*, 14061-14070.

(18) Schlenoff, J. B.; Dubas, S. T. Mechanism of Polyelectrolyte Multilayer Growth: Charge Overcompensation and Distribution. *Macromolecules* **2001**, *34*, 592-598.

(19) Liu, G.; Hou, Y.; Xiao, X.; Zhang, G. Specific Anion Effects on the Growth of a Polyelectrolyte Multilayer in Single and Mixed Electrolyte Solutions Investigated with Quartz Crystal Microbalance. *The Journal of Physical Chemistry B* **2010**, *114*, 9987-9993.

(20) Büscher, K.; Graf, K.; Ahrens, H.; Helm, C. A. Influence of Adsorption Conditions on the Structure of Polyelectrolyte Multilayers. *Langmuir* **2002**, *18*, 3585-3591.

(21) Vikulina, A. S.; Anissimov, Y. G.; Singh, P.; Prokopovic, V. Z.; Uhlig, K.; Jaeger, M. S.; von Klitzing, R.; Duschl, C.; Volodkin, D. Temperature effect on the build-up of exponentially growing polyelectrolyte multilayers. An exponential-to-linear transition point. *Physical Chemistry Chemical Physics* **2016**, *18*, 7866-7874.

(22) Xu, L.; Pristinski, D.; Zhuk, A.; Stoddart, C.; Ankner, J. F.; Sukhishvili, S. A. Linear versus Exponential Growth of Weak Polyelectrolyte Multilayers: Correlation with Polyelectrolyte Complexes. *Macromolecules* **2012**, *45*, 3892-3901.

(23) Bieker, P.; Schönhoff, M. Linear and Exponential Growth Regimes of Multilayers of Weak Polyelectrolytes in Dependence on pH. *Macromolecules* **2010**, *43*, 5052-5059.

(24) Hübsch, E.; Ball, V.; Senger, B.; Decher, G.; Voegel, J.-C.; Schaaf, P. Controlling the Growth Regime of Polyelectrolyte Multilayer Films: Changing from Exponential to Linear Growth by Adjusting the Composition of Polyelectrolyte Mixtures. *Langmuir* **2004**, *20*, 1980-1985.

(25) Haynie, D. T.; Cho, E.; Waduge, P. "In and Out Diffusion" Hypothesis of Exponential Multilayer Film Buildup Revisited. *Langmuir* **2011**, *27*, 5700-5704.

(26) Hoda, N.; Larson, R. G. Modeling the Buildup of Exponentially Growing Polyelectrolyte Multilayer Films. *The Journal of Physical Chemistry B* **2009**, *113*, 4232-4241.

(27) Selin, V.; Ankner, J. F.; Sukhishvili, S. A. Diffusional Response of Layer-by-Layer Assembled Polyelectrolyte Chains to Salt Annealing. *Macromolecules* **2015**, *48*, 3983-3990.

(28) Zhuk, A.; Selin, V.; Zhuk, I.; Belov, B.; Ankner, J. F.; Sukhishvili, S. A. Chain Conformation and Dynamics in Spin-Assisted Weak Polyelectrolyte Multilayers. *Langmuir* **2015**, *31*, 3889-3896.

(29) Zhang, X.; Xia, J. H.; Gaynor, S. G.; Matyjaszewski, K. Atom transfer radical polymerization using functional initiators containing carboxylic acid group. *Abstr. Pap. Am. Chem. S.* **1998**, *216*, U872-U872.

(30) Xu, L.; Ankner, J. F.; Sukhishvili, S. A. Steric Effects in Ionic Pairing and Polyelectrolyte Interdiffusion within Multilayered Films: A Neutron Reflectometry Study. *Macromolecules* **2011**, *44*, 6518-6524.

(31) Dubas, S. T.; Schlenoff, J. B. Factors Controlling the Growth of Polyelectrolyte Multilayers. *Macromolecules* **1999**, *32*, 8153-8160.

(32) Comyn, J.: Introduction to Polymer Permeability and the Mathematics of Diffusion. In *Polymer Permeability*; Comyn, J., Ed.; Springer Netherlands: Dordrecht, 1985; pp 1-10.

(33) Dodoo, S.; Steitz, R.; Laschewsky, A.; von Klitzing, R. Effect of ionic strength and type of ions on the structure of water swollen polyelectrolyte multilayers. *Physical Chemistry Chemical Physics* **2011**, *13*, 10318-10325.

(34) Zerball, M.; Laschewsky, A.; von Klitzing, R. Swelling of Polyelectrolyte Multilayers: The Relation Between, Surface and Bulk Characteristics. *The Journal of Physical Chemistry B* **2015**, *119*, 11879-11886.

(35) Kolasińska, M.; Krastev, R.; Gutberlet, T.; Warszyński, P.: Swelling and Water Uptake of PAH/PSS Polyelectrolyte Multilayers. In *Surface and Interfacial Forces – From Fundamentals to Applications*; Auernhammer, G. K., Butt, H.-J., Vollmer, D., Eds.; Springer Berlin Heidelberg: Berlin, Heidelberg, 2008; pp 30-38.

(36) Kharlampieva, E.; Sukhishvili, S. A. Ionization and pH Stability of Multilayers Formed by Self-Assembly of Weak Polyelectrolytes. *Langmuir* **2003**, *19*, 1235-1243.

(37) Zan, X.; Peng, B.; Hoagland, D. A.; Su, Z. Polyelectrolyte uptake by PEMs: Impact of salt concentration. *Polymer Chemistry* **2011**, *2*, 2581-2589.

(38) Pristinski, D.; Kozlovskaya, V.; Sukhishvili, S. A. Fluorescence correlation spectroscopy studies of diffusion of a weak polyelectrolyte in aqueous solutions. *The Journal of Chemical Physics* **2005**, *122*, 014907.

(39) Jourdainne, L.; Lecuyer, S.; Arntz, Y.; Picart, C.; Schaaf, P.; Senger, B.; Voegel, J. C.; Lavalle, P.; Charitat, T. Dynamics of poly(L-lysine) in hyaluronic acid/poly(L-lysine)multilayer films studied by fluorescence recovery after pattern photobleaching. *Langmuir* **2008**, *24*, 7842-7847.

(40) Owusu-Nkwantabisah, S.; Gammana, M.; Tripp, C. P. Dynamics of Layer-by-Layer Growth of a Polyelectrolyte Multilayer Studied in Situ Using Attenuated Total Reflectance Infrared Spectroscopy. *Langmuir* **2014**, *30*, 11696-11703.

(41) Sukhishvili, S. A.; Granick, S. Layered, Erasable Polymer Multilayers Formed by Hydrogen-Bonded Sequential Self-Assembly. *Macromolecules* **2002**, *35*, 301-310.

(42) Rishard, M. Z. M.; Irwin, R. M.; Laane, J. Vibrational Spectra, DFT Calculations, Unusual Structure, Anomalous CH2 Wagging and Twisting Modes, and Phase-Dependent Conformation of 1,3-Disilacyclobutane. *The Journal of Physical Chemistry A* **2007**, *111*, 825-831.

(43) Korneev, D.; Lvov, Y.; Decher, G.; Schmitt, J.; Yaradaikin, S. Neutron reflectivity analysis of self-assembled film superlattices with alternate layers of deuterated and hydrogenated polysterenesulfonate and polyallylamine. *Physica B: Condensed Matter* **1995**, *213*, 954-956.

(44) Lösche, M.; Schmitt, J.; Decher, G.; Bouwman, W. G.; Kjaer, K. Detailed Structure of Molecularly Thin Polyelectrolyte Multilayer Films on Solid Substrates as Revealed by Neutron Reflectometry. *Macromolecules* **1998**, *31*, 8893-8906.

(45) Kharlampieva, E.; Kozlovskaya, V.; Ankner, J. F.; Sukhishvili, S. A. Hydrogen-Bonded Polymer Multilayers Probed by Neutron Reflectivity. *Langmuir* **2008**, *24*, 11346-11349.

(46) Köhler, R.; Dönch, I.; Ott, P.; Laschewsky, A.; Fery, A.; Krastev, R. Neutron Reflectometry Study of Swelling of Polyelectrolyte Multilayers in Water Vapors: Influence of Charge Density of the Polycation. *Langmuir* **2009**, *25*, 11576-11585.

For Table of Contents Only

Nonlinear Layer-by-Layer Films: Effects of Chain Diffusivity on Film Structure and Swelling

Victor Selin[1], John F. Ankner[2], Svetlana A. Sukhishvili[1]*

[1] *Department of Materials Science & Engineering, Texas A&M University, College Station, Texas 77843, USA*

[2]*Spallation Neutron Source, Oak Ridge National Laboratory, Oak Ridge, Tennessee 37831, USA*